

# Retrograded Eclogite From Chicheng, North China Craton: New Insights Into the Fidelity of U-Pb-Hf-O Isotopes in Zircon During High-grade Metamorphism

Dongya Zou

Zhejiang University

Hongfu Zhang (✉ [hfzhang2020@nwu.edu.cn](mailto:hfzhang2020@nwu.edu.cn))

Zhejiang University

M. Santosh

Northwest University

---

## Research Article

**Keywords:** U-Pb-Hf-O isotopes, Trace elements, Zircon recrystallization, High-grade metamorphism

**Posted Date:** May 26th, 2021

**DOI:** <https://doi.org/10.21203/rs.3.rs-541469/v1>

**License:** © ⓘ This work is licensed under a Creative Commons Attribution 4.0 International License.

[Read Full License](#)

---

# Abstract

Zircon is the most abundantly used mineral for dating igneous and metamorphic events and for tracing source characteristics. Understanding the geochemical behavior of the U-Pb-Hf-O isotope systems during high-grade metamorphism is therefore important for accurate interpretation of the isotopic information. We report zircon U-Pb-Hf-O isotopes and trace elements of retrograded eclogites and host gneisses from Chicheng, North China Craton, with the aim to obtain new insights into the fidelity of U-Pb-Hf-O isotopes in zircon as recorders of high-grade metamorphism. U-Pb dating suggested that the Chicheng mélange experienced eclogite facies metamorphism at  $\sim 1.84$  Ga, and then exhumed to amphibolite facies at 320–300 Ma. Zircons with Paleoproterozoic ages formed in metamorphic melts-derived from the gneiss during the eclogite facies metamorphism. Zircons with ages of 300–320 Ma formed by recrystallization of peak metamorphic zircons during fluid-assisted amphibolite-facies retrograde metamorphism. This process led to the near-complete resetting not only of U-Pb ages but also of Hf-O isotopic compositions of the peak metamorphic zircons, while preserve REE patterns. These results contrast with the sluggish Hf diffusion rate predicted from experimental studies, and support findings that isotopic data from metamorphic zircons in retrograded high-grade metamorphic rocks need not be faithful recorders of their sources.

## Introduction

Zircon is one of the most commonly used minerals for isotopic age determination, because of its occurrence in a wide variety of rocks, and its high U yet low common Pb contents, together with its chemically resistant property<sup>1</sup>. Hf-O isotopes in zircon have been widely used to trace the sources and evolution of rocks<sup>2–4</sup>. However, in high-grade metamorphic rocks with prolonged and complex histories, the U-Pb-Hf-O isotopic compositions determined from zircon grains are less easily interpreted, because zircon shows complex mineralogical and geochemical behavior during high-grade metamorphism<sup>5–8</sup>. Zircon can form either by metamorphic recrystallization from pre-existing magmatic or metamorphic crystals or by new growth in metamorphic fluids/melts during high-grade metamorphism<sup>6–12</sup>. Metamorphic recrystallization of pre-existing zircon can have via processes involving solid-state diffusion-reaction or dissolution-reprecipitation<sup>5–9</sup>. Both processes can cause resetting of U-Pb ages and O isotope, and weak disturbance of Hf isotope systems, and the different isotopic systems exhibit disparate behavior during metamorphism<sup>13–15</sup>. The Pb, Hf and O diffusion rates in crystalline zircon were shown to be sluggish under anhydrous conditions<sup>16–20</sup>, whereas O diffuses faster under hydrous conditions<sup>16,21</sup>. In addition, the resetting of U-Pb ages is also controlled by the degree of radiation damage of the zircon lattice<sup>10,22</sup>, which variably resets U-Pb ages when zircon recrystallization without fluids<sup>5,13,14</sup>. In contrast, during dissolution-reprecipitation and recrystallization in the presence of metamorphic fluids, both U-Pb ages and O isotope system in zircon would be partially or completely reset<sup>13,14</sup>. Several studies have demonstrated that Hf isotopes, once incorporated into zircon, would not be fractionated or only weakly disturbed during later metamorphic processes ranging from solid-state recrystallization to dissolution-reprecipitation<sup>13–15,23–25</sup>. However, in this study, we found that not only U-

Pb ages and O isotopes but also Hf isotopes in recrystallized metamorphic zircon were totally reset by intense fluid-assisted amphibolite-facies retrograde metamorphism. We present an integrated study of U-Pb-Hf-O isotopes and trace elements in zircons from the retrograded eclogites and surrounding gneisses from the Chicheng region within the Trans-North China Orogen (TNCO) of the North China Craton (NCC). This provides a new baseline for an informed interpretation of U-Pb ages and Hf-O isotopic information obtained from metamorphic zircon grains in high-grade rocks.

## Geological background and samples

The Chicheng mélangé is located at the northern margin of the TNCO of the NCC (Fig. 1a). The TNCO is a Paleoproterozoic collisional orogen along which the Eastern and Western Blocks of the NCC amalgamated at 1.85–1.95 Ga<sup>26–28</sup>. The Chicheng mélangé mainly comprises retrograded eclogite, serpentized peridotites and amphibole-plagioclase gneisses. The retrograded eclogites and serpentized peridotites are exposed as tectonic lenses within the gneisses of the Archean Hongqiyingzi complex (Fig. 1b), which are interpreted as parts of Late Archean-Early Paleoproterozoic oceanic lithosphere<sup>29–31</sup>. The gneisses represent meta-volcano-sedimentary units<sup>30,31</sup>, and the retrograded eclogites and peridotites represent fragments of tholeiitic oceanic crust<sup>32</sup> and sub-oceanic lithospheric mantle, respectively<sup>29,33</sup>. Together, they experienced eclogite-facies metamorphism at 1.85–1.80 Ga<sup>30,31</sup>, and then exhumed to amphibolite facies at 326–300 Ma<sup>31,34,35</sup>. Abundant retrograded eclogite lenses occur within gneisses in the Qilidun village, Chicheng country (Fig. 1b), which show a size range of 4–50 m (Fig. 1c). The host gneisses are composed of quartz, plagioclase, garnet, amphibole and minor biotite (Fig. 1d). The retrograded eclogites are composed of garnet, amphibole, and plagioclase with minor rutile and ilmenite (Fig. 1e). Some garnet grains are surrounded or completely replaced by symplectitic amphibole-plagioclase kelyphitic rims (Fig. 1e).

## Results

Representative cathodoluminescence (CL) images of zircon grains are shown in Fig. 2 together with U-Pb ages. Zircons from the Chicheng gneiss and retrograded eclogite display no or patchy zoning structures with grey-dark CL brightness (Figs. 2A-E). A summary of U-Pb-Hf-O isotopic and trace element compositions of the zircon grains in the Chicheng gneiss and retrograded eclogites is provided in Tables S1 and S2 in Supplementary Information, respectively.

A total of 43 zircon grains from the wall-rock gneiss CC14-08 were analyzed for their isotopic compositions. Thirty-seven zircons with dark CL brightness (Fig. 2A) yield apparent <sup>207</sup>Pb/<sup>206</sup>Pb ages from 1635 to 1892 Ma, defining an upper intercept age of 1840 ± 10 Ma (Fig. 2a). They have high Th (92.7–963 ppm) and U contents (217–1222 ppm), high Th/U ratios (0.10–1.51) (Fig. 3a) and large range of ε<sub>Hf</sub>(t) (-7.4 to -0.5) (Figs. 3b and 4) and δ<sup>18</sup>O (+9.4 to +14.6) (Fig. 3c). The other six zircons with patchy structure and grey CL brightness yield a concordia age of 301 ± 9 Ma (Fig. 2a), with low Th (0.043–0.786 ppm) and U contents (14.8–97.9 ppm), Th/U ratios (0.003–0.019) (Fig. 3a) and δ<sup>18</sup>O (+9.6

to + 10.3) (Fig. 3c), and large ranges of  $\epsilon_{\text{Hf}}(t)$  (-36.5 to -0.3) (Fig. 3b). 24 zircons have enough spaces for trace element analyses. Zircons with Paleoproterozoic ages show positive Ce anomalies and negative Eu anomalies, and low contents of MREE and HREE relative to the protolith zircons (Fig. 5a). Some grains show flat HREE pattern with  $(\text{Lu}/\text{Gd})_{\text{N}}$  values of 0.665–2.71 (Table S2 and Fig. 5a), others display shallow MREE-HREE patterns and high  $(\text{Lu}/\text{Gd})_{\text{N}}$  values of 10.8–31.1 (Table S2 and Fig. 5a). They have Ti contents of 11.7–38.8 ppm to yield Ti-in-zircon temperatures of 755–876°C (Table S2). Zircons with ages of 300–320 Ma have similar REE patterns with zircons of ~ 1.8 Ga (Fig. 5a), but obvious lower Ti contents of 1.37–8.91 ppm and Ti-in-zircon temperatures of 592–731°C (Table S2).

A total of 18 zircon grains from retrograded eclogite sample CC14-01 were analyzed. Among these, two grains with dark CL property (Fig. 2B) have the oldest apparent  $^{207}\text{Pb}/^{206}\text{Pb}$  ages of 1845 and 1811 Ma (Fig. 2b), respectively, with high Th (324–456 ppm) and U contents (840–1126 ppm), high Th/U ratios (0.36–0.60) (Fig. 3a) and  $\delta^{18}\text{O}$  (+ 13.8 to + 14.1) (Fig. 3c), and low  $\epsilon_{\text{Hf}}(t)$  (-1.5 to -3.5) (Fig. 3b). The other 16 grains yield a concordia age of  $317 \pm 1$  Ma (Fig. 2b) with low Th (0.509–4.59 ppm) and U contents (147–737 ppm), Th/U ratios (0.003–0.014) (Fig. 3a) and  $\delta^{18}\text{O}$  (+ 11.6 to + 12.5) (Fig. 3c), and variable  $\epsilon_{\text{Hf}}(t)$  (-4.0 to + 14.8) (Fig. 3b). They together define an upper intercept age of  $1837 \pm 10$  Ma (Fig. 2b). Trace elements analyses were not obtained for the smaller grain of zircon.

Most zircons in sample CC14-10 (total n = 59 grains) are similar to those with young ages from CC14-01, but seven grains display obvious core-rim structure (Fig. 2C). The cores show resorption texture and replacement by the unzoned zircon rims. In addition, the cores have many mineral and fluid inclusions observed in transmitted light (Fig. 2C). Among sixty-five spot analyses (Table S1), seven cores yield older apparent ages of 321–1494 Ma (Fig. 2c), with relatively high Th contents (46.8–370 ppm) and Th/U ratios (0.11–1.02) (Fig. 3a), and substantial variation of  $\epsilon_{\text{Hf}}(t)$  values (-26.4 to 12.8) (Fig. 3b) and  $\delta^{18}\text{O}$  (+ 4.55 to + 9.64) (Fig. 3c). Five analyzable broader rims of zircon with core-rim texture and another 52 zircons without core-rim structure together yield a concordia age of  $305 \pm 2$  Ma (Fig. 2c), with low Th contents (0.385–7.56 ppm) and Th/U (0.005–0.031) (Fig. 3a), and large ranges of  $\epsilon_{\text{Hf}}(t)$  (-4.5 to + 8.8) (Fig. 3b) and  $\delta^{18}\text{O}$  (+ 10.6 to + 12.2) (Fig. 3c). 27 zircons with ages of 300–320 Ma have enough spaces for trace elements analyses. They show low and flat HREE pattern with  $(\text{Lu}/\text{Gd})_{\text{N}}$  values of 1.10–4.57 (Table S2 and Fig. 5b), and have Ti contents of 0.958–12.4 ppm and Ti-in-zircon temperatures of 570–760°C (Table S2).

Zircons from retrograded eclogite samples CC14-06 and CC14-07 have similar isotopic compositions. Seventy-four spot analyses were made on 66 zircon grains from sample CC14-06. They yield a concordia age of  $314 \pm 1$  Ma (Fig. 2d) with low Th contents (0.124–9.71 ppm), Th/U ratios (0.002–0.069) (Fig. 3a), and various  $\epsilon_{\text{Hf}}(t)$  (+ 0.5 to + 17.5) (Fig. 3b) and  $\delta^{18}\text{O}$  (+ 10.0 to + 11.5) (Fig. 3c). Thirty-seven spot analyses were made on 31 zircon grains from sample CC14-07. They yield a concordia age of  $315 \pm 3$  Ma (Fig. 2e) with low Th contents (0.327–15.6 ppm), Th/U ratios (0.005–0.086) (Fig. 3a), and varying  $\epsilon_{\text{Hf}}(t)$  (+ 6.7 to + 14.0) (Fig. 3b) and  $\delta^{18}\text{O}$  (+ 10.3 to + 11.5) (Fig. 3c). 59 and 20 spot analyses of trace elements

were made for samples CC14-06 and CC14-07, respectively. They show flat HREE pattern with  $(\text{Lu}/\text{Gd})_N$  values of 0.517–11.04 (Table S2 and Figs. 5c and d). They have Ti contents of 0.705–10.3 ppm and 1.19–4.95 ppm, yielding Ti-in-zircon temperatures of 551–743°C and 583–683°C, respectively (Table S2).

## Discussion

The symplectites consisting of fine-grained plagioclase and amphibole formed around or completely replace the garnet grains in the Chicheng retrograded eclogites (Fig. 1e). These observations suggest that they experienced amphibolite facies retrograde metamorphism following early-stage eclogite facies metamorphism, as previously reported<sup>32</sup>. The Paleoproterozoic ages of ~ 1.84 Ga from the upper intercept ages of wall-rock gneiss (Fig. 2a) and one retrograded eclogite (Fig. 2b) are consistent with previous results which suggest that the eclogite facies metamorphism for the Chicheng mélange possibly occurred at 1.80–1.85 Ga<sup>30, 31, 38</sup>. This event is also consistent with the formation timing of TNCO<sup>26–28</sup>. Moreover, zircons with Paleoproterozoic ages show significant lower HREE contents than the protolith zircon of gneiss from the Sulu orogen (Fig. 5a)<sup>24</sup>. Flat HREE patterns of some zircons (Fig. 5a) suggest that they formed in the presence of garnet<sup>24, 39, 40</sup>. Some zircons have shallow MREE-HREE patterns, suggesting insignificant effect of garnet<sup>24</sup>, but they still have lower HREE contents than the protolith zircons (Fig. 5a). Therefore, zircon grains with age of ~ 1.84 Ga formed during the eclogite facies metamorphism of the Chicheng gneiss and eclogite, which is also consistent with the higher Ti-in-zircon temperatures of 755–876°C (Table S2).

Conversely, zircons in the wall-rock gneiss and four retrograded eclogite samples give concordia ages of 301, 317, 305, 314 and 315 Ma (Fig. 2), respectively, which is in accordance with the previous results that show an age range of 300–326 Ma<sup>31, 32, 34, 35</sup> and the <sup>40</sup>Ar/<sup>39</sup>Ar age (~ 331 Ma) of amphibole from the Chicheng retrograded eclogite<sup>35</sup>. Therefore, we suggest that zircons with apparent ages of 300–320 Ma record amphibolite facies retrograde metamorphism. However, some zircon cores from sample CC14-10 yield ages from 320 to 1494 Ma (Fig. 2c). These cores were possibly influenced by amphibolite facies retrograde metamorphism, resulting in partial resetting of the U-Pb ages to different degrees. The irregular relict cores show spongy texture (Fig. 2C) as those observed in zircon that underwent dissolution recrystallization, while the rims exhibit no zoning<sup>13, 40</sup>. These pairs of core-rim structure may form by dissolution recrystallization, in which the cores and rims represent the inclusion-rich and pure domains, respectively<sup>24</sup>. Thus, the U-Pb ages of zircon cores from the sample CC14-10 do not have geological meaning, and deviate from the previously suggested protolith ages<sup>32, 34</sup>.

In high-grade metamorphic rocks, zircon can form either by recrystallization from pre-existing magmatic or metamorphic crystals or by new growth in metamorphic fluids/melts during metamorphism<sup>6–12</sup>. The gneisses and retrograded eclogites in this study experienced a polyphase evolution, with peak metamorphism in the Paleoproterozoic and amphibolite facies retrograde metamorphism upon exhumation at ~ 320–300 Ma. In the following, combined petrographic and geochemical information are used to distinguish between these various origins for zircons from the Chicheng gneiss and retrograded

eclogites: (1) Zircon structure, (2) Th, U contents and Th/U ratios obtained from U-Pb geochronology, (3) Hf-O isotopic composition and (4) trace element compositions.

The unzoned or patchy zoned structures (Figs. 2A-E) of zircons from Chicheng gneiss and retrograded eclogites reflect their metamorphic origin. The grains with peak metamorphic age might have crystallized from metamorphic melts with higher Th and U contents and Th/U ratios (Fig. 3a), as suggested in previous studies<sup>11, 12</sup>. The similar lower  $\epsilon_{\text{Hf}}(t)$  (Fig. 3b) and higher  $\delta^{18}\text{O}$  (Fig. 3c) in zircons with peak metamorphic age from the gneiss and retrograded eclogite suggest that the metamorphic melts could be from the wall-rock gneiss during the eclogite facies metamorphism. The interpretation is compatible with the wall-rock gneiss representing the uppermost meta-sedimentary unit within the ophiolitic mélange on the continental margin<sup>29, 41</sup>, which could have elevated  $\delta^{18}\text{O}$  (up to 19.2)<sup>42</sup>.

In contrast to zircons with Paleoproterozoic ages, zircon grains with ages of 300–320 Ma have low Th contents and Th/U (< 0.1) (Fig. 3a). One explanation is that U is more fluid-mobile than Th under conditions that are oxidizing enough for some water-soluble  $\text{U}^{6+}$  to be present<sup>43</sup>. This is taken to indicate the formation of these zircons in the presence of fluids<sup>5</sup>. In addition, the observations that garnets are replaced by symplectite of amphibole and plagioclase in Chicheng retrograded eclogites (Fig. 1e), and the occurrence of fluid inclusions in zircon cores from sample CC14-10 (Fig. 2C), suggest extensive fluids activities during the amphibolite facies retrograde metamorphism<sup>23, 44</sup>. Metamorphic fluids can be liberated from eclogite via decompression exsolution of structural hydroxyl and molecular water during exhumation<sup>45–47</sup>. The higher  $\epsilon_{\text{Hf}}(t)$  in zircons with ages of 300–320 Ma (Figs. 3b and 4) imply that the metamorphic fluids were characterized by high  $^{176}\text{Hf}/^{177}\text{Hf}$  ratios, which could result from garnet breakdown during retrograde metamorphism<sup>13, 23</sup>. During zircon growth by breakdown of garnet, the  $^{176}\text{Hf}/^{177}\text{Hf}$  ratio for the newly grown zircon would be elevated<sup>48</sup>. The  $\delta^{18}\text{O}$  in zircons with ages of 300–320 Ma fall in the field for the altered oceanic crust (Fig. 3c), which could be the protolith of Chicheng retrograded eclogite. The geochemical composition of the Chicheng retrograded eclogite indicates that their igneous precursors were oceanic basalts<sup>32</sup>, which should have normal mantle  $\delta^{18}\text{O}$  value. During subsequent pervasive hydrothermal alteration by seawater,  $\delta^{18}\text{O}$  values are enriched in the oceanic basalts (8.2–12.7)<sup>36</sup>. Thus, this also supports the notion that the metamorphic fluids were derived from the eclogite during the amphibolite facies retrograde metamorphism.

However, the large ranges of Hf-O isotopic compositions in zircons with ages of 300–320 Ma suggest that they are not simple new growth grains in the metamorphic fluids, but could be recrystallization of pre-existing zircons. Alternatively, or in addition, Hf-O isotopes were disturbed during interaction with the metamorphic fluid. Fluids would increase the O diffusion rates in zircon<sup>16</sup>, and act as a catalyzer for the healing of radiation-damages zircon<sup>5, 49, 50</sup>. The  $\epsilon_{\text{Hf}}(t)$  show obvious negative relationship with  $\delta^{18}\text{O}$  in zircons with U-Pb ages of 300–320 Ma from the retrograded eclogites (Fig. 4). This might imply that the degree of modification of Hf-O isotopic compositions in pre-existing zircons increases with increased accessibility to eclogite-derived fluids with radiogenic Hf and light O. Zircons formed by dissolution-

recipitation recrystallization of pre-existing zircon in a closed system, the isotopic compositions would be the weighted mean values of the pre-existing zircons and fluids derived from the matrix, e.g., garnet<sup>13, 15, 23</sup>. In this scenario, the initial Hf isotope ratios of the peak metamorphic zircons from the gneiss and retrograded eclogite are calculated at  $t = 301$  and  $t = 317$  Ma, respectively. The result indicates that the Hf-O isotopic compositions of zircons with ages of 300–320 Ma could be mixing between peak metamorphic zircons and metamorphic fluids-derived from the eclogite (Fig. 4). Therefore, dissolution-recipitation recrystallization of peak metamorphic zircons during amphibolite facies retrograde metamorphism would have resulted in the complete resetting of U-Pb ages and Hf-O isotopes in peak metamorphic zircons. Zircons with ages of 300–320 Ma from the wall-rock gneiss have lower and more variable  $\epsilon_{\text{Hf}}(t)$  from  $-36.5$  to  $-0.3$  (Fig. 4), and zircons with peak metamorphic ages show large variations of  $\delta^{18}\text{O}$  but almost constant  $\epsilon_{\text{Hf}}(t)$  (Fig. 4). These observations imply that zircons from the gneiss were weakly affected by the metamorphic fluids during the retrograde metamorphism, which only lead to the resetting of U-Pb ages and  $\delta^{18}\text{O}$  to different degrees but did not or minimally disturb the Hf isotopic compositions.

Zircon with ages of 300–320 Ma and Paleoproterozoic have similar trace element compositions (Fig. 5a), and most of zircon with ages of 300–320 Ma show flat HREE patterns (Figs. 5b-d). This also implies that the 300–320 Ma zircons could have been formed by recrystallization of peak metamorphic zircons during amphibolite-facies retrograde metamorphism. Zircon recrystallization is commonly characterized by the preservation of the REE signature of the precursor due to their lower diffusion rates<sup>16, 18</sup>. The decoupled variation between Pb and REE in zircons during the amphibolite-facies retrograde metamorphism has been observed in other studies of Dabie-Sulu orogen belt<sup>14, 24, 39, 40</sup>.

Hafnium isotopic compositions are considered as the most robust system relative to U-Pb and O during high-grade metamorphism because of the slower diffusion rate of Hf under dry conditions<sup>16, 19</sup>. In addition, previous studies have suggested that the Hf isotopes in zircon are not or only minimally disturbed during the solid and dissolution recrystallization process<sup>13–15, 23–25</sup>. However, our study of zircons from the Chicheng retrograded eclogite indicates that not only the U-Pb ages and O isotopic compositions of peak metamorphic zircon could be completely reset, but also the Hf isotopic compositions can be strongly altered during the retrograde metamorphism assisted by extensive fluids. Thus, we speculate that the Hf diffusion rate is not so sluggish under hydrous conditions, as previously considered<sup>19</sup>. Therefore, the U-Pb ages and Hf-O isotopic information in zircons obtained from the high-grade metamorphic rocks need to be interpreted with caution.

## Methods

Zircon O-U-Pb isotope analyses were performed using the same Cameca IMS1280 at Institute of Geology and Geophysics in Chinese Academy of Sciences (IGGCAS) following the methods described by<sup>51</sup>. The  $\text{Cs}^+$  primary ion beam was accelerated at 10 kV, with an intensity of  $\sim 2$  nA and rastered over a  $10 \mu\text{m}$  area, and with spot about  $20 \mu\text{m}$  in diameter for oxygen isotopic measurement. The  $\text{O}^{2-}$  beam was

accelerated at 13 kV, with an intensity of  $\sim 8\text{--}10$  nA and ellipsoidal spot of ca.  $20\times 30$   $\mu\text{m}$  in size for U-Pb geochronology. The instrumental mass fractionation factor (IMF) was corrected using zircon 91500 as a reference. Two working zircon reference materials “Qinghu” and “Penglai” were used to monitor the machine stability. The reproducibility of the two reference samples was better than 0.26‰, and the internal precision of a single analysis was generally better than 0.2‰. Values of  $\delta^{18}\text{O}$  were standardized to VSMOW.

Lu-Hf isotopes and trace element compositions were conducted using the Geolas 193 nm laser coupled to a Neptune Plasma II multi-collector inductively coupled plasma mass spectrometry (MC-ICP-MS) and an Agilent 7500 inductively coupled plasma–mass spectrometry (ICP–MS), respectively, at the State Key Laboratory of Continental Dynamics, Northwest University, Xi’an, China. The laser was operated at a nominal ablation diameter of 40  $\mu\text{m}$ , repetition rate of 8 Hz and laser beam energy density of 10 J/cm<sup>2</sup>. Details of the technique are described in<sup>52, 53</sup>. If space allowed, all analyses were placed in the same zircon domain, as shown in CL images.

## Declarations

### Acknowledgements

This research was financially supported by the National Natural Science Foundation of China (Grant 41688103 and 42003026). We thank Aulbach, Sonja for editorial handling and discussions that helped to improve the manuscript.

### Author Contributions

D.Y.Z. and H.F.Z. conducted the fieldwork. D.Y.Z. conducted the U-Pb-Hf-O isotopes and trace elements analyses. All authors contributed to writing the paper.

### Competing Interests

The authors declare no competing interests.

## References

1. U. Schärer, C. Allègre, Uranium-lead system in fragments of a single zircon grain. *Nature* **295**, 585-587 (1982).
2. Tsuyoshi, Iizuka, Takao, Yamaguchi, Keita, Itano, Yuki, Hibiya, Kazue, Suzuki, What Hf isotopes in zircon tell us about crust–mantle evolution. *Lithos* **274-275**, 304-327 (2017).
3. J. Valley, J. Chiarenzelli, J. McLelland, Oxygen isotope geochemistry of zircon. *Earth and Planetary Science Letters* **126**, 187-206 (1994).
4. M. Van Kranendonk, C. Kirkland, J. Cliff, Oxygen isotopes in Pilbara Craton zircons support a global increase in crustal recycling at 3.2 Ga. *Lithos* **228-229**, 90-98 (2015).

5. W. Geisler, Thorsten, U. Schaltegger, F. Tomaschek, Re-equilibration of Zircon in Aqueous Fluids and Melts. *Elements* **3**, 43-50 (2007).
6. U. Schaltegger, C. Fanning, D. Günther, J. Maurin, K. Schulmann, D. Gebauer, Growth, annealing and recrystallization of zircon and preservation of monazite in high-grade metamorphism: Conventional and in-situ U-Pb isotope, cathodoluminescence and microchemical evidence. *Contributions to Mineralogy and Petrology* **134**, 186-201 (1999).
7. P. W. O. Hoskin, L. P. Black, Metamorphic zircon formation by solid-state recrystallization of protolith igneous zircon. *Journal of Metamorphic Geology* **18**, 423-439 (2001).
8. M. Tichomirowa, M. J. Whitehouse, L. Nasdala, Resorption, growth, solid state recrystallisation, and annealing of granulite facies zircon - A case study from the Central Erzgebirge, Bohemian Massif. *Lithos* **82**, 25-50 (2005).
9. M. Schidlowski, Recrystallization of Zircon as an Indication of Contact Metamorphism. *Nature* **197**, 68-69 (1963).
10. R. Pidgeon, Recrystallisation of oscillatory zoned zircon: some geochronological and petrological implications. *Contributions to Mineralogy and Petrology* **110**, 463-472 (1992).
11. H. Yu, H. F. Zhang, X. H. Li, J. Zhang, M. Santosh, Y. H. Yang, D. W. Zhou, Tectonic evolution of the North Qinling Orogen from subduction to collision and exhumation: Evidence from zircons in metamorphic rocks of the Qinling Group. *Gondwana Research* **30**, (2015).
12. Q. X. Xia, Y. F. Zheng, H. L. Yuan, F. Y. Wu, Contrasting Lu-Hf and U-Th-Pb isotope systematics between metamorphic growth and recrystallization of zircon from eclogite-facies metagranites in the Dabie orogen, China. *Lithos* **112**, 477-496 (2009).
13. Y. F. Zheng, Y. B. Wu, Z. F. Zhao, S. B. Zhang, P. Xu, F. Y. Wu, Metamorphic effect on zircon Lu-Hf and U-Pb isotope systems in ultrahigh-pressure metagranite and metabasite. *Earth and Planetary Science Letters* **240**, 378-400 (2005).
14. Y. X. Chen, Y. F. Zheng, R. X. Chen, S. B. Zhang, Q. L. Li, M. M. Dai, L. Chen, Metamorphic growth and recrystallization of zircons in extremely 18O-depleted rocks during eclogite-facies metamorphism: Evidence from U-Pb ages, trace elements, and O-Hf isotopes. *Geochimica et Cosmochimica Acta* **75**, 4877-4898 (2011).
15. Y. M. Sheng, Y. F. Zheng, R. X. Chen, Q. L. Li, M. M. Dai, Fluid action on zircon growth and recrystallization during quartz veining within UHP eclogite: Insights from U-Pb ages, O-Hf isotopes and trace elements. *Lithos* **136-139**, 126-144 (2012).
16. D. Cherniak, E. B. Watson, Diffusion in Zircon. *Reviews in Mineralogy & Geochemistry* **53**, 113-143 (2003).
17. J. Lee, I. Williams, D. Ellis, Pb, U and Th diffusion in natural zircon. *Nature* **390**, 159-162 (1997).
18. L. Martin, S. Duchêne, E. Deloule, O. Vanderhaeghe, Mobility of trace elements and oxygen in zircon during metamorphism: Consequences for geochemical tracing. *Earth and Planetary Science Letters* **267**, 161-174 (2008).

19. D. Cherniak, J. Hanchar, E. Watson, Diffusion of Tetravalent Cations in Zircon. *Beiträge zur Mineralogie und Petrographie* **127**, 383-390 (1997).
20. D. Cherniak, E. Watson, Pb Diffusion in zircon. *Chemical Geology* **172**, 5-24 (2001).
21. N. Roberts, Q.-Y. Yang, M. Santosh, Rapid oxygen diffusion during high temperature alteration of zircon. *Scientific Reports* **8**, 3661 (2018).
22. A. Anderson, J. Hanchar, K. Hodges, M. van Soest, Mapping radiation damage zoning in zircon using Raman spectroscopy: Implications for zircon chronology. *Chemical Geology* **538**, 119494 (2020).
23. Y. B. Wu, Y. F. Zheng, Z. F. Zhao, B. Gong, X. M. Liu, F. Y. Wu, U-Pb, Hf and O isotope evidence for two episodes of fluid-assisted zircon growth in marble-hosted eclogites from the Dabie orogen. *Geochimica et Cosmochimica Acta* **70**, 3743-3761 (2006).
24. R. X. Chen, Y. F. Zheng, L. W. Xie, Metamorphic growth and recrystallization of zircon: Distinction by simultaneous in-situ analyses of trace elements, U–Th–Pb and Lu–Hf isotopes in zircons from eclogite-facies rocks in the Sulu orogen. *Lithos* **114**, 132-154 (2010).
25. M. Flowerdew, I. Millar, A. Vaughan, M. Horstwood, C. Fanning, The source of granitic gneisses and migmatites in the Antarctic Peninsula: A combined U-Pb SHRIMP and laser ablation Hf isotope study of complex zircons. *Contributions to Mineralogy and Petrology* **151**, 751-768 (2006).
26. G. C. Zhao, P. A. Cawood, S. Li, S. A. Wilde, M. Sun, J. Zhang, Y. H. He, C. Q. Yin, Amalgamation of the North China Craton: Key issues and discussion. *Precambrian Research* **222-223**, 55-76 (2012).
27. G. Zhao, M. Sun, S. Wilde, L. Sanzhong, Late Archean to Paleoproterozoic evolution of the North China Craton: Key issues revisited. *Journal of Asian Earth Sciences* **24**, 519-522 (2005).
28. M. Santosh, Assembling North China Craton within the Columbia supercontinent: The role of double-sided subduction. *Precambrian Research* **178**, 149-167 (2010).
29. H. Liu, H. F. Zhang, Paleoproterozoic ophiolite remnants in the northern margin of the North China Craton: Evidence from the Chicheng peridotite massif. *Lithos* **344**, 311-323 (2019).
30. H. Liu, H. F. Zhang, M. Santosh, Neoproterozoic growth and Paleoproterozoic metamorphism of an Archean ophiolite mélange in the North China Craton. *Precambrian Research* **331**, 105377 (2019).
31. Y. Y. Zhang, C. J. Wei, H. Chu, Paleoproterozoic oceanic subduction in the North China Craton: Insights from the metamorphic P–T–t paths of the Chicheng Mélange in the Hongqiyingzi Complex. *Precambrian Research* **342**, 105671 (2020).
32. Z. Y. Ni, M. G. Zhai, R. M. Wang, Y. Tong, Late Paleozoic retrograded eclogites from within the northern margin of the North China Craton: Evidence for subduction of the Paleo-Asian ocean. *Gondwana Research* **9**, 209-224 (2006).
33. W. Tian, S. Y. Wang, F. L. Liu, Z. Y. Chu, B. Wang, Archean-Paleoproterozoic Lithospheric Mantle at the Northern Margin of the North China Craton Represented by Tectonically Exhumed Peridotites. *Acta Geologica Sinica* **91**, 2041-2057 (2017).
34. H. Chu, H. C. Wang, C. J. Wei, H. Liu, S. N. Lu, Y. W. Ren, J. R. Zhang, Geochronology of the Paleozoic metamorphism in the Chicheng area, north Hebei, and its geological significance. *Acta Geologica*

- Sinica* **87**, 1233–1246 (in Chinese with English abstract) (2013).
35. X. Kong, Z. Y. Ni, M. G. Zhai, Y. R. Shi, G. Yan, J. Zhang, Time sequence of evolution for the retrograde eclogite from Chicheng, Northern Hebei province: Evidence from zircon Shrimp U-Pb dating. *Journal of Mineralogy and Petrology* **31**, 15-22 (in Chinese with English abstract) (2011).
  36. R. T. Gregory, H. P. Taylor, An oxygen isotope profile in a Section of Cretaceous Oceanic Crust Samail Ophiolite, Oman: Evidence for  $\delta^{18}\text{O}$  Buffering of the Oceans by Deep (>5 km) Seawater-Hydrothermal Circulation at Mid-Ocean Ridges. *Journal of Geophysical Research* **86**, 2737-2755 (1981).
  37. C. Chauvel, E. Lewin, M. Carpentier, N. T. Arndt, J. Marini, Role of recycled oceanic basalt and sediment in generating the Hf–Nd mantle array. *Nature Geoscience* **1**, 64-67 (2008).
  38. H. F. Zhang, D. Y. Zou, M. Santosh, B. Zhu, Phanerozoic orogeny triggers reactivation and exhumation in the northern part of the Archean–Paleoproterozoic North China Craton. *Lithos* **261**, 46-54 (2015).
  39. K. Q. Zong, Y. S. Liu, C. G. Gao, Z. C. Hu, S. Gao, H. J. Gong, In situ U-Pb dating and trace element analysis of zircons in thin sections of eclogite: Refining constraints on the ultra high-pressure metamorphism of the Sulu terrane, China. *Chemical Geology* **269**, 237-251 (2010).
  40. F. L. Liu, A. Gerdes, P. H. Liu, U-Pb, trace element and Lu-Hf properties of unique dissolution-precipitation zircon from UHP eclogite in SW Sulu terrane, eastern China. *Gondwana Research* **22**, 169-183 (2012).
  41. J. Zhang, Z. Y. Ni, M. G. Zhai, J. S. Lu, G. Yan, X. K. X. Zhou, Petrology, geochemistry and protolith of the biotite plagiogneiss from Hongqiyangzi Group in Chicheng County, northern Hebei Province. *Acta Petrologica et Mineralogica* **31**, 307-322 (in Chinese with English abstract) (2012).
  42. H. Staudigel, G. R. Davies, S. R. Hart, K. M. Marchant, Large scale isotopic Sr, Nd and O isotopic anatomy of altered oceanic crust: DSDP/ODP sites 417/418. *Earth and Planetary Science Letters* **130**, 169-185 (1995).
  43. H. Liu, R. E. Zartman, T. R. Ireland, W. D. Sun, Global atmospheric oxygen variations recorded by Th/U systematics of igneous rocks. *Proceedings of the National Academy of Sciences* **116**, 18854-18859 (2019).
  44. Y. F. Zheng, Y. B. Wu, F. K. Chen, B. Gong, L. Li, Z. F. Zhao, Zircon U-Pb and oxygen isotope evidence for a large-scale  $^{18}\text{O}$  depletion event in igneous rocks during the Neoproterozoic. *Geochimica et Cosmochimica Acta* **68**, 4145-4165 (2004).
  45. B. Yardley, S. Gleeson, S. Bruce, Origin of retrograde fluids in metamorphic rocks. *Journal of Geochemical Exploration* **69**, 281-285 (2000).
  46. R. X. Chen, Y. F. Zheng, B. Gong, Z. F. Zhao, T. S. Gao, B. Chen, Y. B. Wu, Origin of retrograde fluid in ultrahigh-pressure metamorphic rocks: constraints from mineral hydrogen isotope and water content changes in eclogite-gneiss transitions in the Sulu orogen. *Geochimica et Cosmochimica Acta* **71**, 2299–2325 (2007).
  47. Z. F. Zhao, B. Chen, Y. F. Zheng, R. X. Chen, Y. B. Wu, Mineral oxygen isotope and hydroxyl content changes in ultrahigh-pressure eclogite–gneiss contacts from Chinese Continental Scientific Drilling Project cores. *Journal of Metamorphic Geology* **25**, 165-186 (2007).

48. A. Gerdes, A. Zeh, Zircon formation versus zircon alteration – New insights from combined U-Pb and Lu-Hf in-situ La-ICP-MS analyses of Archean zircons from the Limpopo Belt. *Chemical Geology* **261**, 230-243 (2009).
49. C. Schmidt, Low-temperature Zr mobility: An in situ synchrotron-radiation XRF study of the effect of radiation damage in zircon on the element release in H<sub>2</sub>O + HCl SiO<sub>2</sub> fluids. *American Mineralogist* **91**, 1211-1215 (2006).
50. T. Geisler, K. Trachenko, S. Ríos, M. Dove, E. Salje, Impact of self-irradiation damage on the aqueous durability of zircon (ZrSiO<sub>4</sub>): Implications for its suitability as a nuclear waste form. *Journal of Physics: Condensed Matter* **15**, L597 (2003).
51. X. H. Li, W. X. Li, Q. L. Li, X. C. Wang, Y. Liu, Y. H. Yang, Petrogenesis and tectonic significance of the ~850 Ma Gangbian alkaline complex in South China: Evidence from in situ zircon U–Pb dating, Hf–O isotopes and whole-rock geochemistry. *Lithos* **114**, 1-15 (2010).
52. Z. A. Bao, H. L. Yuan, C. L. Zong, L. Ye, K. Y. Chen, Y. L. Zhang, Simultaneous Determination of Trace Elements and Lead Isotopes in Fused Silicate Rock Powders Using a Boron Nitride Vessel and fsLA-(MC)-ICP-MS. *Journal of Analytical Atomic Spectrometry* **31**, 1012-1022 (2016).
53. H. L. Yuan, S. Gao, M. N. Dai, C. L. Zong, D. Günther, G. Fontaine, C. R. Diwu, Simultaneous determinations of U-Pb age, Hf isotopes and trace element compositions of zircon by excimer laser-ablation quadrupole and multiple-collector ICP-MS. *Chemical Geology* **247**, 100-118 (2008).

## Figures

**Fig. 1**

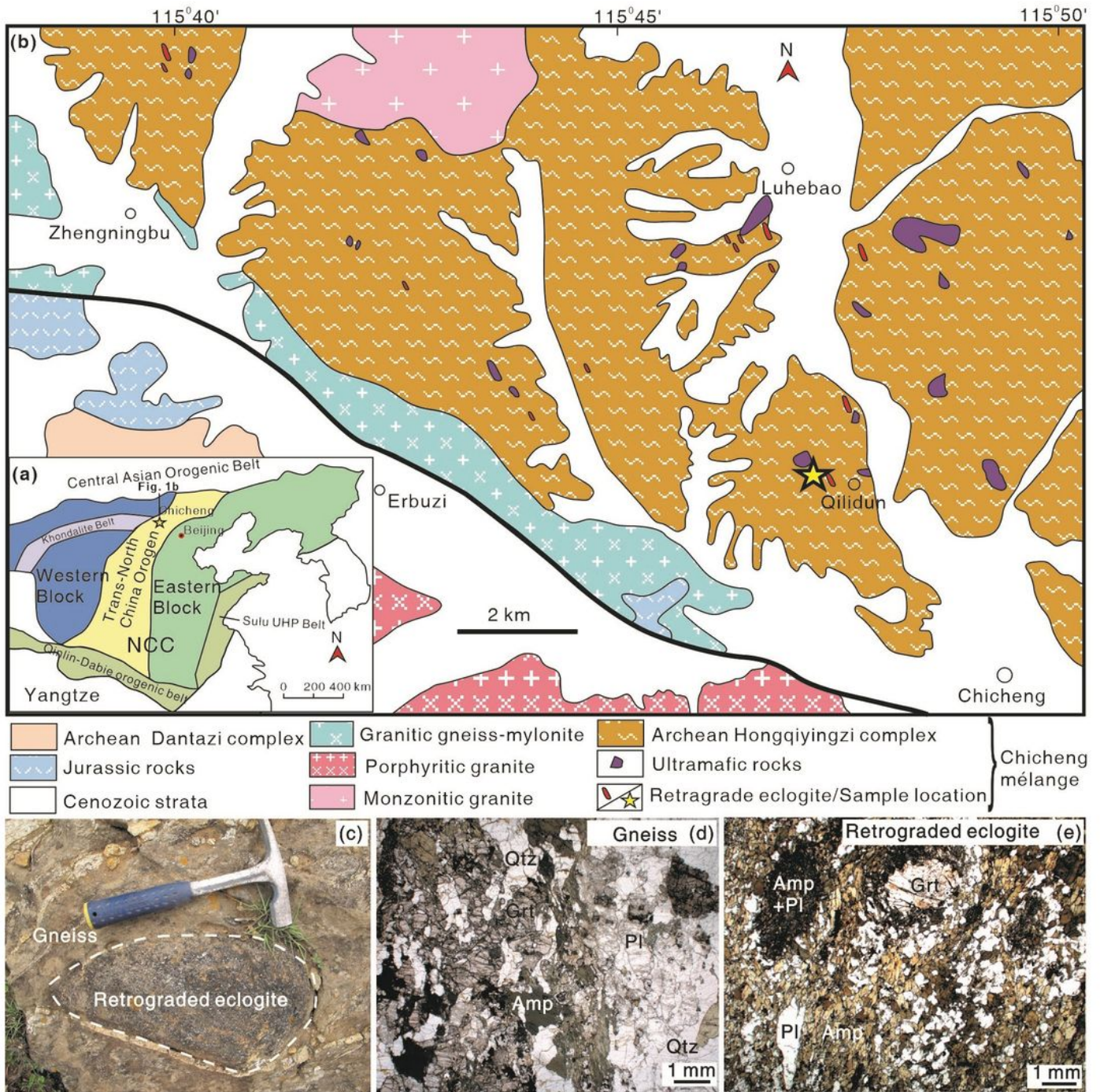


**Figure 1**

(a) Tectonic subdivision of the North China Craton (NCC), modified from 27. (b) Geological map showing the details of the Chicheng mélangé and sample locality. (c) Field photographs of outcrops showing retrograde eclogite lenses within gneiss. (d) Photomicrograph of the gneiss showing the main mineral assemblage of quartz (Qtz), garnet (Grt), plagioclase (Pl) and amphibole (Amp). (e) Photomicrograph of the retrograded eclogite showing the main mineral assemblage of Grt, Amp and Pl. Note: The

designations employed and the presentation of the material on this map do not imply the expression of any opinion whatsoever on the part of Research Square concerning the legal status of any country, territory, city or area or of its authorities, or concerning the delimitation of its frontiers or boundaries. This map has been provided by the authors.

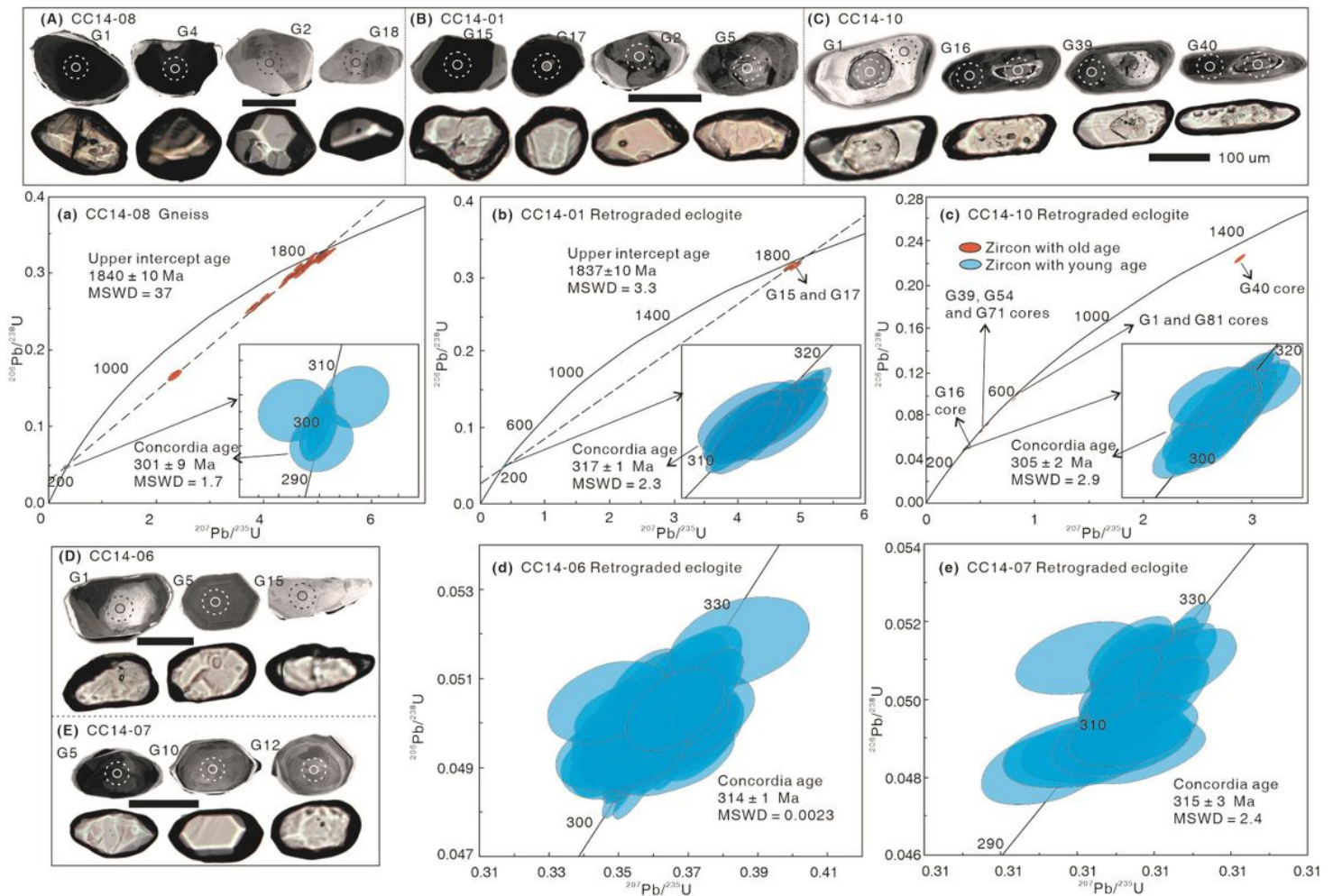


**Figure 2**

(A-E) Cathodoluminescence images and corresponding transmitted light photographs of representative zircon grains, and (a-e) U-Pb Concordia diagrams for the wall-rock gneiss and retrograded eclogite from Chicheng region. (A) and (a) for CC14-08, (B) and (b) for CC14-01, (C) and (c) for CC14-10, (D) and (d) for CC14-06, and (E) and (e) for CC14-07. The small dotted circles and large solid circles on the zircons represent the analyze positions for O-U-Pb isotopes and Hf isotopes, respectively.

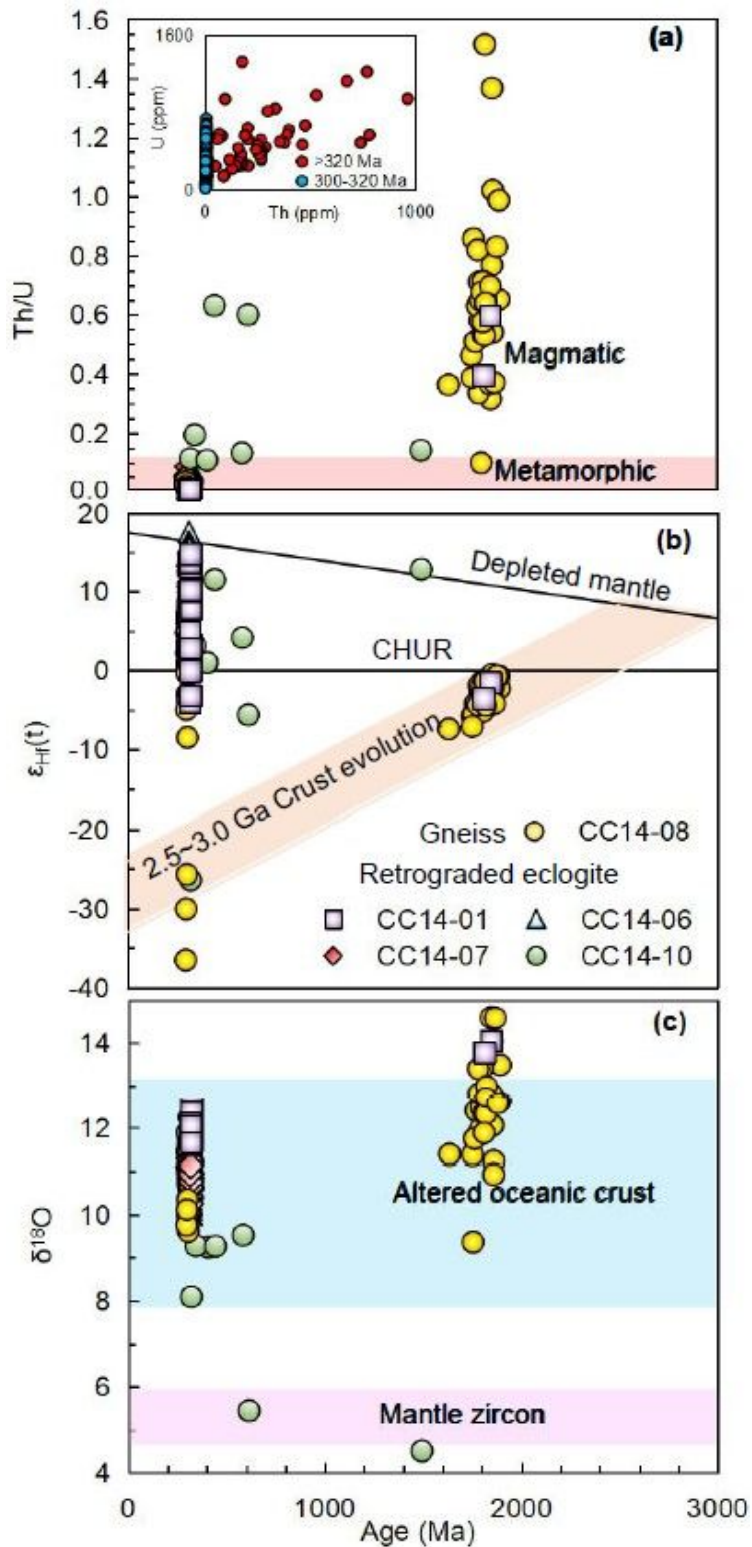


**Figure 3**

(a) Th/U ratios, (b)  $\epsilon_{\text{Hf}}(t)$  and (c)  $\delta^{18}\text{O}$  versus U-Pb ages in zircons from Chicheng gneiss and retrograded eclogite. Plot of Th versus U contents in zircons is showed in the (a). Fields for the  $\delta^{18}\text{O}$  of mantle zircon and altered oceanic crust are from 3 and 36, respectively.

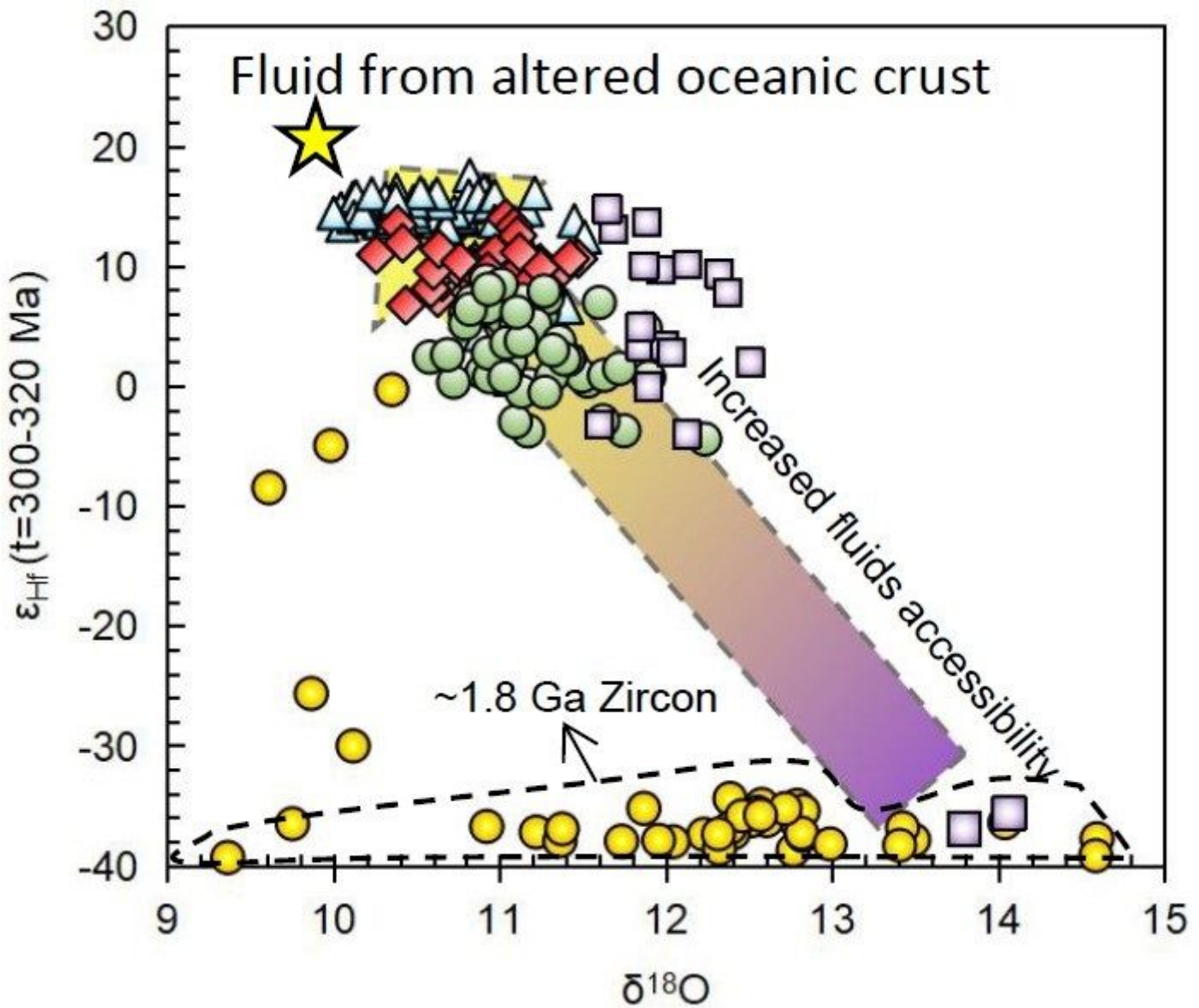
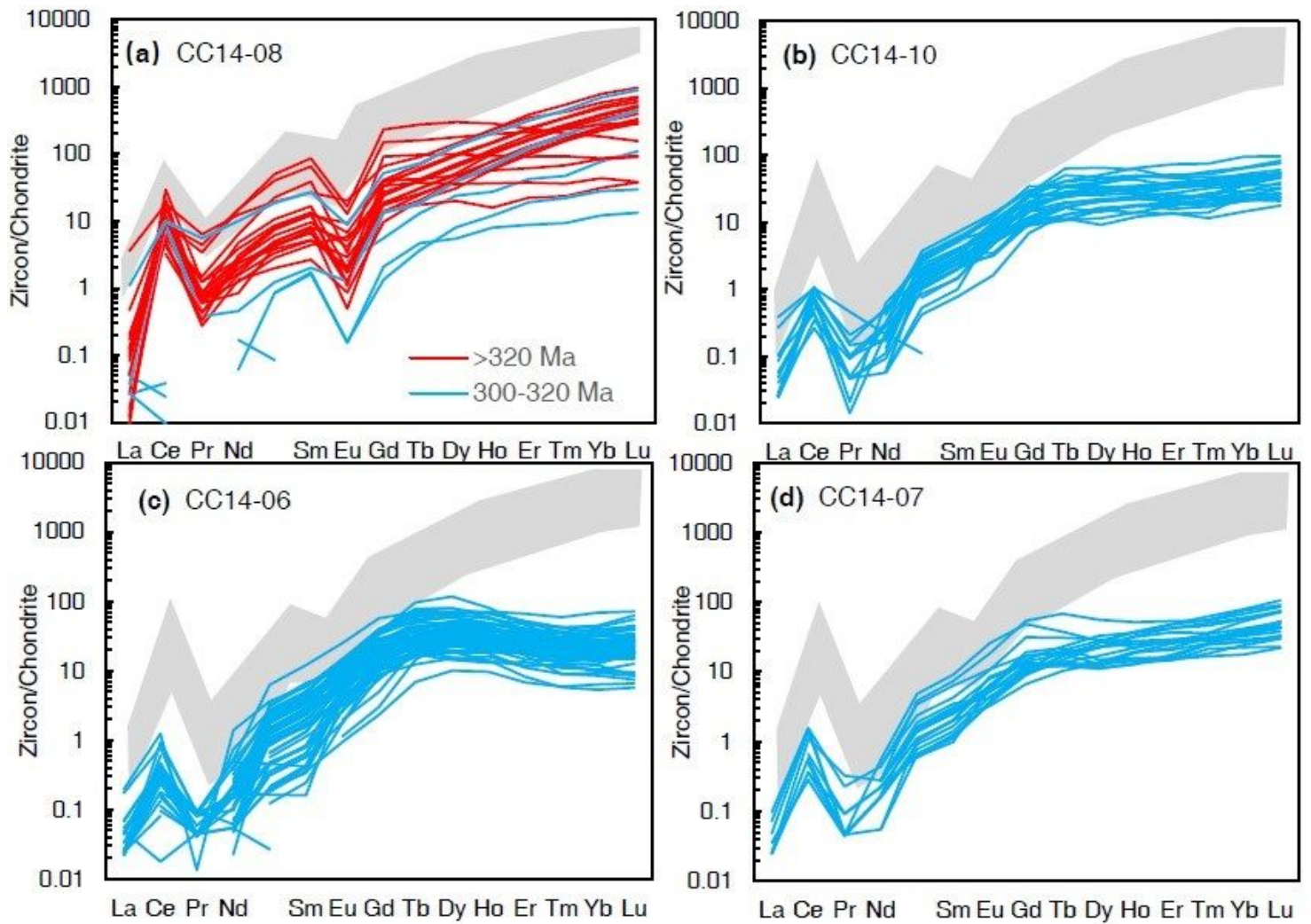


Figure 4

$\epsilon_{\text{Hf}}(t)$  versus  $\delta^{18}\text{O}$  in zircon grains from Chicheng gneiss and retrograded eclogite. The initial Hf isotope ratios of zircon with age of  $\sim 1.84$  Ga from gneiss and retrograded eclogite are calculated at  $t = 301$  Ma and  $t = 317$  Ma, respectively.  $\epsilon_{\text{Hf}}(t = 310 \text{ Ma})$  and  $\delta^{18}\text{O}$  values of fluid from altered oceanic crust (i.e., protolith of eclogite) are from 37 and 36, respectively.



**Figure 5**

Chondrite-normalized REE patterns of zircon from Chicheng gneiss and retrograded eclogite. Grey zones in (a) and (b-d) represent the REE patterns of protolith zircon of gneiss and eclogite from CCSD-MH in the Sulu orogen<sup>24</sup>, respectively.

## Supplementary Files

This is a list of supplementary files associated with this preprint. Click to download.

- [SupplementaryTables.pdf](#)